Journal of Biomedical Optics

BiomedicalOptics.SPIEDigitalLibrary.org

5-aminolevulinic acid for quantitative seek-and-treat of high-grade dysplasia in Barrett's esophagus cellular models

Shu-Chi Allison Yeh
Celine S. N. Ling
David W. Andrews
Michael S. Patterson
Kevin R. Diamond
Joseph E. Hayward
David Armstrong
Qiyin Fang

SPIE.

5-aminolevulinic acid for quantitative seek-and-treat of high-grade dysplasia in Barrett's esophagus cellular models

Shu-Chi Allison Yeh,[a] Celine S. N. Ling,[b] David W. Andrews,[c] Michael S. Patterson,[d] Kevin R. Diamond,[d] Joseph E. Hayward,[d] David Armstrong,[e] and Qiyin Fang[a,b,*]
[a]McMaster University, School of Biomedical Engineering, 1280 Main Street West, Hamilton, Ontario, L8S 4K1 Canada
[b]McMaster University, Department of Engineering Physics, 1280 Main Street West, Hamilton, Ontario, L8S 4K1 Canada
[c]Sunnybrook Research Institute, 2075 Bayview Avenue, Toronto, Ontario, M4N 3M5 Canada
[d]McMaster University, Department of Medical Physics and Applied Radiation Sciences, 1280 Main Street West, Hamilton, Ontario, L8S 4K1 Canada
[e]McMaster University, Division of Gastroenterology, Department of Medicine, 1280 Main Street West, Hamilton, Ontario, L8S 4K1 Canada

Abstract. High-grade dysplasia (HGD) in Barrett's esophagus (BE) poses increased risk for developing esophageal adenocarcinoma. To date, early detection and treatment of HGD regions are still challenging due to the sampling error from tissue biopsy and relocation error during the treatment after histopathological analysis. In this study, CP-A (metaplasia) and CP-B (HGD) cell lines were used to investigate the "seek-and-treat" potential using 5-aminolevulinic acid-induced protoporphyrin IX (PpIX). The photodynamic therapy photosensitizer then provides both a phototoxic effect and additional image contrast for automatic detection and real-time laser treatment. Complementary to our studies on automatic classification, this work focused on characterizing subcellular irradiation and the potential phototoxicity on both metaplasia and HGD. The treatment results showed that the HGD cells are less viable than metaplastic cells due to more PpIX production at earlier times. Also, due to mitochondrial localization of PpIX, a better killing effect was achieved by involving mitochondria or whole cells compared with just nucleus irradiation in the detected region. With the additional toxicity given by PpIX and potential morphological/textural differences for pattern recognition, this cellular platform serves as a platform to further investigate real-time "seek-and-treat" strategies in three-dimensional models for improving early detection and treatment of BE. © *2015 Society of Photo-Optical Instrumentation Engineers (SPIE)* [DOI: 10.1117/1.JBO.20.2.028002]

Keywords: Barrett's esophagus; photodynamic therapy; 5-aminolevulinic acid; PpIX; subcellular treatment.

Paper 140687R received Oct. 18, 2014; accepted for publication Jan. 13, 2015; published online Feb. 11, 2015.

1 Introduction

Barrett's esophagus (BE) is a precancerous condition occurring in the lower esophagus, where the original squamous epithelium undergoes metaplastic transformation and is replaced by the intestinalized columnar cells.[1,2] BE can progress through low-grade dysplasia to high-grade dysplasia (HGD), which significantly increases the risk of developing esophageal adenocarcinoma if early treatment is not provided.[3–5] Although various interventions have been studied extensively,[6–11] the diagnostic techniques are still inadequate and suspected areas of HGD may be missed because of sampling errors for the initial biopsies or because of an inability to locate the same target areas on repeat endoscopy. This is a common problem because pathological analysis following four-quadrant biopsy is the current gold standard for evaluating suspected lesions. Because it can take several days to process, stain, and examine the biopsies, diagnosis and treatment are commonly separated into two steps, which leads to difficulties in accurate relocalization of the lesions in separate procedures.[4] Optical biopsy is an emerging technique that takes advantages of the distinct tissue optical properties of targeted lesions to enable real-time diagnosis.[12] In particular, the cellular-based optical biopsy retrieves subcellular Barrett's-associated characteristics by the use of point spectroscopy or endomicroscopy.[4,13] However, there are substantial challenges in detecting dysplasia in BE with optical biopsy including poor signal-to-noise ratio, low specificity in fluorescence endoscopy imaging[14] and significant patient-to-patient variability.[4] To address these challenges, microscopic-based visualization of subcellular morphology with the addition of an exogenous contrast agent is desirable to enhance the contrast between normal, metaplastic, and HGD regions. Fluorescence of photosensitizers used in photodynamic therapy (PDT) has been reported to be beneficial in distinguishing drug–cellular interactions, giving PDT photosensitizers additional merits besides being therapeutic reagents.[15] Using fluorescence from FDA-approved photosensitizers as a contrast agent becomes an attractive option for clinical translation of the techniques.[16,17] In addition, the use of photosensitizers may provide additional treatment efficacy. In other words, integrated detection and treatment can be achieved using well-characterized light illumination immediately following a robust detection with quantitative feature extraction and classification. Palanca-Wessels et al. have developed metaplasia (CP-A) and HGD (CP-B, CP-C, and CP-D) cell strains from BE.[18] The morphological features and cellular behaviors of these cell lines have been investigated along with normal squamous epithelial cells in both coculture and organotypic culture models.[18–20] Therefore, these cell lines could potentially serve as a cellular-based platform to study the integrated early detection and treatment of BE.

*Address all correspondence to: Qiyin Fang, E-mail: qiyin.fang@mcmaster.ca

1083-3668/2015/$25.00 © 2015 SPIE

In this study, we have focused on characterizing the subcellular irradiation efficacies in order to understand the potential protoporphyrin IX (PpIX) phototoxicity on both metaplasia and HGD cell lines after detection. The microscopic images obtained at subcellular resolution would be comparable with microendoscopic technologies in development.[13,21,22] Among potential PDT "contrast agents," 5-aminolevulinic acid (5-ALA) is an endogenous heme precursor that localizes well in mucosal tissues.[10] It produces preferential accumulation of cytotoxic PpIX at the mitochondrial membranes,[23,24] which can potentially lead to treatment selectivity; more importantly, PpIX provides the nucleus contrast for detection of HGD.[13] To date, although 5-ALA has been studied extensively for treating BE *in vivo*, limited selectivity was noted for dysplastic cells.[11,25–30] Our goal is to use the BE cellular platform to investigate the feasibility of integrated detection and treatment. The quantitative imaging analysis, feature extraction, and classification performance have been investigated in our group,[31] followed by the characterization of localized, subcellular treatment efficacy in this study to examine the optimal irradiation scheme.

2 Materials and Methods

We characterized the dose response curves of two BE cell lines (CP-A and CP-B) to various doses of light fluence using one-photon and two-photon irradiations. Three irradiation regimes that target the whole cell, mitochondria, and cell nuclei were applied at each light dose in order to investigate the treatment efficacy as a result of targeted subcellular PDT. Experiments were conducted in the presence or absence of 5-ALA for positive and negative controls.

2.1 *Cell Culture*

CP-A (nondysplastic metaplasia, ATCC® CRL-4027™, American Type Culture Collection, Manassas, Virginia) and CP-B (HGD, ATCC® CRL-4028™) are both hTERT-immortalized epithelial cells derived from human esophagus.[18] These well-characterized premalignant cell lines were selected as an *in vitro* platform to study subcellular treatment efficacy. Both cell lines were cultured under identical conditions using the same batch of MCDB 153 base medium (M7403, Sigma, St. Louis, Missouri), supplemented with 5% fetal bovine serum (16000-036, Gibco®, Life Technologies, Burlington, Ontario, Canada), 0.25 μg/ml Amphotericin B (A2942, Sigma), 1% penicillin/streptomycin (15140-122, Gibco®), 0.4 μg/ml hydrocortisone (H0888, Sigma), 140 μg/ml bovine pituitary extract (P1476, Sigma), 20 mg/L Adenine (A8626, Sigma), 0.1% insulin-transferrin-sodium selenite (I1884, Sigma), 20 ng/ml Recombinant EGF (E9644, Sigma), 4 mM glutamine (G7513, Sigma), and 1 nM cholera toxin (C8052, Sigma). Cells were maintained at 37°C in a water-jacketed CO_2 incubator (Forma Series II, Thermo Fisher Scientific Inc., Waltham, Massachusetts) and passaged as recommended by ATCC. All experimental data were acquired using cells within 10 passages after cryopreservation to minimize the variability due to cell degradation.[32]

2.2 *Experimental Preparation*

In this study, 5-ALA (A3785, Sigma) served as a fluorescent marker as well as a PDT photosensitizer. A stock solution of 100 mM 5-ALA dissolved in PBS (14190-144, Gibco®) was prepared and stored in 1 ml aliquots in the dark. Fresh photosensitizer-containing medium was prepared by further diluting the stock solution in the serum-free complete culture medium to a working concentration of 0.5 mM that provides sufficient contrast without yielding dark toxicity.

Cells were detached from a 25 cm^2 culture flask with 2.5× Trypsin-EDTA solutions (0.5%, 15400-054, Gibco®). A centrifugation process at 125g was used to resuspend cells in fresh trypsin-free culture medium. A total of 1×10^5 cells were seeded on a gridded glass-bottom dish (P35G-2-14-CGRD, MatTek, Ashland, Massachusetts) 24 h before the experiment. The culture medium was then replaced by the 0.5-mM 5-ALA-containing medium for a specified incubation period before the experiment. Samples were rinsed with Hanks balanced salt solution (14025-092, Gibco®) supplemented with 20 mM of Hepes buffer (15630-106, Gibco®) before imaging and were immersed in 1 mL of Hanks-Hepes buffer during the imaging acquisition procedures.

2.3 *Imaging Acquisition*

The fluorescence emission of 5-ALA-induced PpIX was collected by a laser scanning confocal microscope (TSC SP5 and DMI 6000 B, Leica, Wetzlar, Germany) equipped with an argon-ion laser operating at 514 nm for one-photon irradiation and a femtosecond Ti:sapphire laser (Chameleon-Ultra, Coherent, Santa Clara, California) pulsing at 810 nm for two-photon excitation. The emission spectral band was set as 600 to 750 nm to maximize the detected PpIX intensity, in combination with a transmitted light detector to acquire bright field images.

2.4 *Subcellular Treatment*

Both cell lines were incubated with 5-ALA for 3 h before imaging and subcellular treatment. The light fluence levels used for imaging and dose response curves are summarized in Table 1, where the fluence was calculated based on the average power (P) measured at the sample plane, total exposure time (t), and the field of view (FOV): 246×246 μm^2. In order to understand the cytotoxic roles played by light fluence and PpIX and eventually to select an appropriate ablative approach, the dose response curves were compared between three treatment schemes selected manually based on the bright field and 5-ALA images using the built-in software of the microscope:

Table 1 Parameters of light doses applied to cell imaging (*) and dose response curves.

One-photon excitation		Two-photon excitation	
P (μW) × t (s)	Fluence (J/cm^2)	P (mW) × t (s)	Fluence (J/cm^2)
0.15 × 6.4	0.002*	45 × 1.28	124*
28 × 5.12	0.24	45 × 5.12	495
70 × 10.24	1.18	45 × 25.6	2478
70 × 25.6	2.96	45 × 51.2	4955
70 × 51.2	5.92	45 × 102.4	9910

Note: Asterisks mean that the fluence used for imaging acquisition is 0.002 J/cm^2.

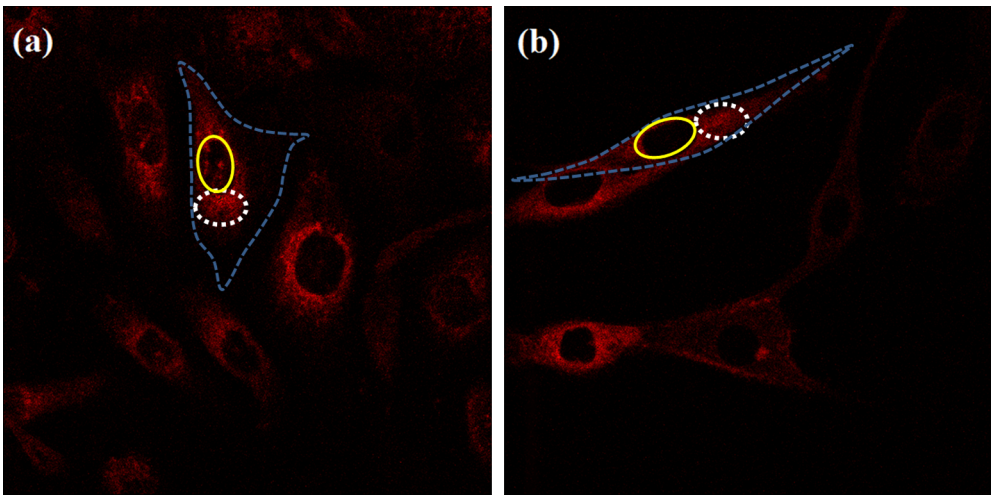

Fig. 1 Sample protoporphyrin IX (PpIX) fluorescence images of metaplastic (CP-A) and high-grade dysplasia (HGD) (CP-B) cells: (a) CP-A cells were incubated with 5-aminolevulinic acid (ALA) for 6 h. (b) CP-B cells were incubated with 5-ALA for 3 h. The red pseudocolor at the mitochondria was PpIX fluorescence excited by an Argon ion laser at 514 nm and collected at the spectral range between 600 and 750 nm. Cell regions selected for photodynamic therapy (PDT) treatment were highlighted, including cell nuclei (solid line), partial mitochondria (dotted line), and the whole cell region that can be visualized in bright field images (dashed line).

(1) Nucleus treatment: only cell nuclei were illuminated; (2) Mitochondrial treatment: only a portion of the perinuclear region highlighted by PpIX was irradiated, with the size of the irradiation field being similar to its cell nucleus; (3) Whole cell treatment: the light was applied through the whole FOV without any selection. The irradiated areas are demonstrated in Fig. 1. All treatment schemes were applied at the focal plane of the cells only, which focused on the center section of approximately 1 μm in thickness. To compare the treatment efficacy after various regimes, a cell viability dye, propidium iodide (PI) (P3566, Life Technologies), at a working concentration of 300 ng/mL was used to stain the nuclei of cells which had a compromised cell membrane at 2 h after the initial irradiation. The fluorescence intensity from PI was collected using the excitation light at 488 nm in combination with the emission range of 600 to 700 nm. Therefore, dead cells are highlighted by PI, and the cell viability was obtained based on the ratio of the remaining cells (nonstained by PI) to the original cell count in the same FOV indicated by the gridded dish. Cell counts were obtained with the highlight of PpIX fluorescence in the experimental groups or using the bright field images in the control groups. Cells were grown to a density that precluded cell overlap to yield accurate counting results.

3 Results

3.1 *Fluorescence of Protoporphyrin IX*

Sample PpIX fluorescence images of metaplastic (CP-A) and HGD (CP-B) cells are shown in Fig. 1. Differences in cell line morphology were observed when cell mitochondria were highlighted by PpIX; CP-A cells showed dense mitochondrial distribution close to the perinuclear region demonstrating a rounder shape, while the mitochondria of CP-B cells spread out through the cells demonstrating a more elongated morphology. Maximum PpIX synthesis typically occurs within 6 h of incubation.[27] It is noted that PpIX intensity in CP-B at 3 h of incubation is comparable with that in CP-A at 6 h of incubation, indicating a faster PpIX synthesis in CP-B cells. Further analysis of the cellular fluorescence images identified a small set of morphological and textural features that differentiated metaplastic (CP-A) and dysplastic (CP-B) cells with a sensitivity of 95% and specificity of 87%, yielding an area under the curve of 0.95 for the receiver operating characteristics curve.[31]

3.2 *Subcellular Irradiation*

Light treatment was given at 3 h after 5-ALA incubation, where the metaplastic and HGD cells exhibited significantly different intracellular PpIX intensity[31] (photon counts of 32 ± 3 in CP-B and 23 ± 2 in CP-A, $p < 0.01$) in our imaging analysis study (data not shown). We employed various regimes to investigate and characterize their treatment efficacy, which could be relevant when the cellular-based treatment or ablation is integrated with endomicroscopic technology. Figures 2–5 demonstrate the dose response curves of CP-B (HGD) and CP-A (metaplasia) cells to various laser irradiation doses using 514 nm (Figs. 2 and 3) or 810 nm (Figs. 4 and 5) irradiations and the cell survival rate associated with three subcellular treatment approaches.

Since both drug and light contribute to cell toxicity, the following comparisons of PDT treatment responses were made: (1) the dose responses of different cell lines, (2) the dose responses of subcellular treatment, (3) 5-ALA and control groups without drug administration, and (4) the effect of one-photon and two-photon illuminations.

When comparing the dose response between two different cell lines incubated with 5-ALA (Fig. 2), it was observed that the HGD cells (CP-B) exhibited a significantly lower survival rate than CP-A cells when the light fluence is greater than 2.96 J/cm^2 ($p < 0.01$): CP-B cells showed an approximately 20% reduction in viability comparing with CP-A cells when using either mitochondria or whole cell treatment. When a light fluence of 5.92 J/cm^2 was given, CP-B cells were observed to be 37% and 51% less viable than CP-A cells with the mitochondria and whole cell treatment, respectively. These facts suggested the dysplastic cell line was more sensitive to the treatment. The

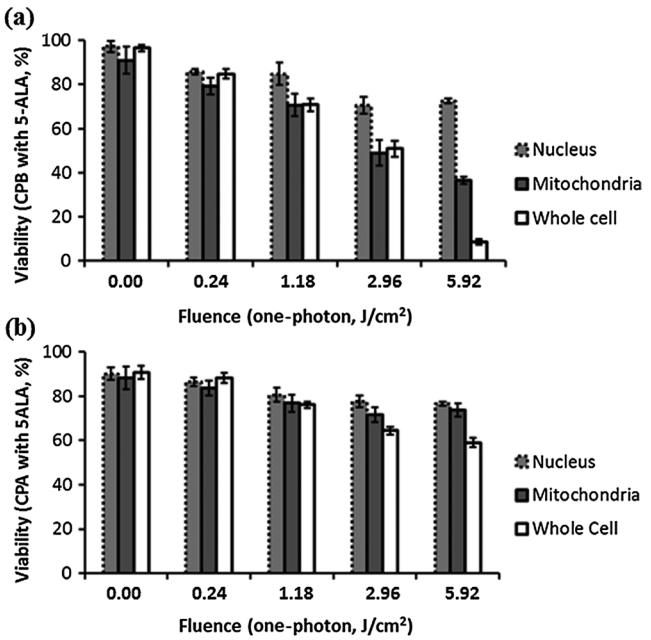

Fig. 2 Cell survival rates of (a) HGD and (b) metaplasia cells after various subcellular treatment regimes were plotted against five laser irradiation fluences operating at 514 nm, ranging from the fluence for imaging acquisition (0.002 J/cm^2) to 5.92 J/cm^2. It was observed that CP-B cells exhibited lower survival rate than CP-A cells when the light fluence is greater than 2.96 J/cm^2, and CP-B cells had up to 50% less viability than CP-A cells when the whole cell area was irradiated. Subcellular treatment also yielded a range of phototoxicity. The reduction of cell viability using 5.92 J/cm^2 was due to the total energy deposition at the "nonstained" cell nuclei, and a similar trend was seen between cell lines. When intracellular PpIX was partially activated in the mitochondria and whole cell PDT regimes, it yielded better CP-B killing efficacy and the cell viability was inversely proportional to the area of activated PpIX (Table 2). Error bars in all figures represent weighted standard deviation from three repetitive trials of each set.

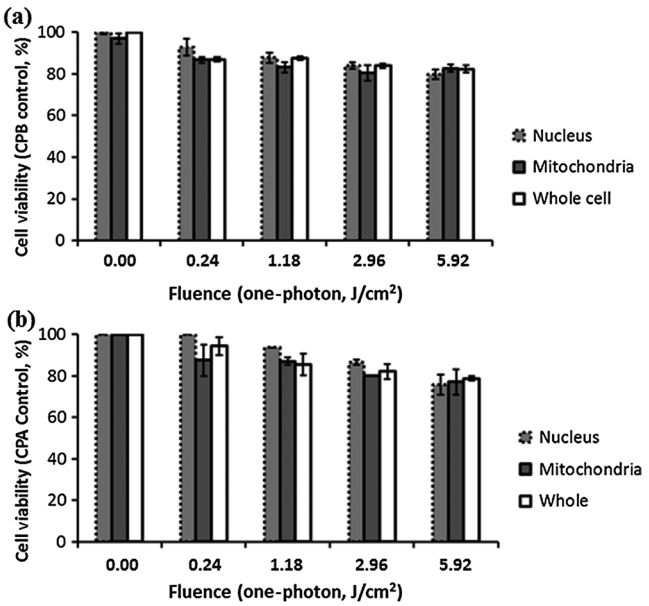

Fig. 3 Cell survival rates of nonstained (a) HGD and (b) metaplasia cells after various subcellular treatment regimes were plotted against five laser irradiation fluence levels operating at 514 nm, ranging from the dose of imaging acquisition (0.002 J/cm^2) to 5.92 J/cm^2. Both cell lines showed equal responses to laser doses with approximately 80% viability after being exposed to the light fluence of 5.92 J/cm^2. A small and reproducible amount of phototoxicity was seen between light doses, which is consistent with the viability reduction of nucleus treatment in Fig. 1.

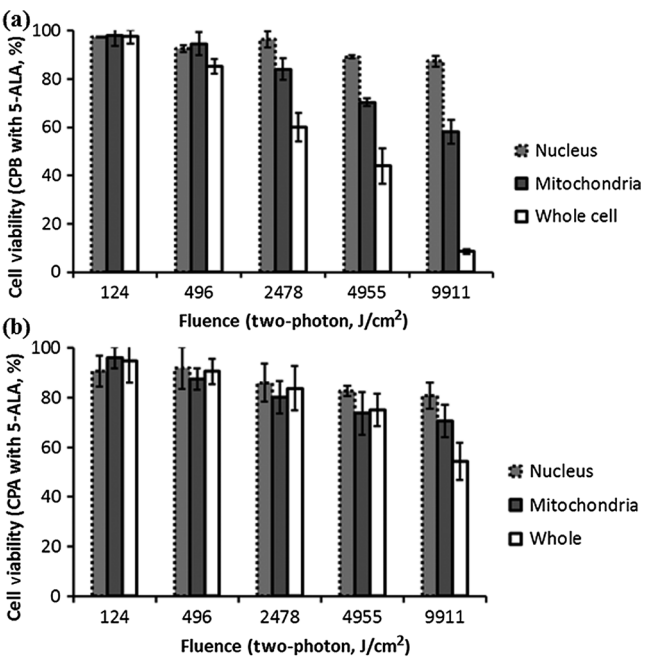

Fig. 4 (a) HGD and (b) metaplasia cells after various subcellular treatment regimes were plotted against five fluence levels operating at 810 nm, ranging from the dose for imaging acquisition (124 J/cm^2) to 9911 J/cm^2. The results agreed with 1-photon treatment, where CP-B cells are more susceptible to PpIX phototoxicity.

proportional cytotoxic contribution from the light irradiation and the photosensitizer will be discussed further when comparing 5-ALA groups with control groups.

Various extents of phototoxic effects from subcellular PDT treatment were also observed. In general, when cells were incubated with 5-ALA, whole cell and mitochondrial irradiations yielded better efficacy when compared with nucleus treatment. This trend is obvious when the light dose is higher than 2.96 J/cm^2 for CP-B ($p < 0.01$) and 5.92 J/cm^2 in CP-A ($p < 0.01$). These results indicate that the irradiation regime involving mitochondria (PpIX location) may enhance the treatment efficacy in HGD while keeping most of metaplasia cells unharmed. For example, when mitochondria of CP-B and CP-A were both irradiated with light at 5.92 J/cm^2, CP-B cells were observed to be less viable ($p < 0.01$). This selectivity may be further enhanced when integrated with quantitative feature extraction and detection.

The dose response curves were also collected using cells without 5-ALA administration (Fig. 3). The results observed from nonstained CP-A and CP-B cells indicated that both cell lines had equivalent responses to the photothermal and photochemical laser effects in no-drug controls. Both cell lines were observed to have greater than 80% of viability with good morphological appearance after being exposed to the high fluence of 5.92 J/cm^2, indicating that the light-induced photochemical and photothermal reactions at this level corresponded to approximately 20% cell death, with no difference observed between cell lines and subcellular regimes ($p > 0.05$). In other words, when comparing the results with 5-ALA groups, 20% of cell deaths caused by mitochondrial

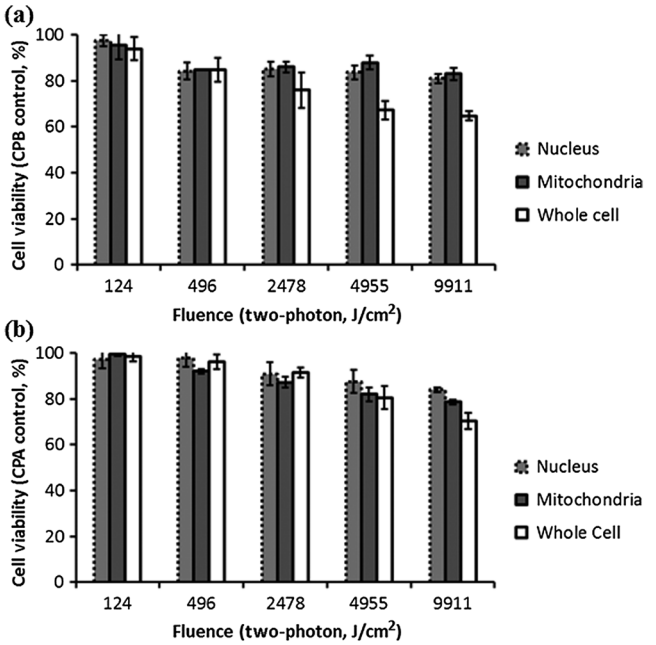

Fig. 5 (a) Nonstained HGD and (b) metaplasia cells after various subcellular treatment regimes were plotted against five fluence levels operating at 810 nm.

and whole cell treatments was attributed to the laser effect, which agrees with the observed 20% cell deaths from the nucleus-only treatment in the 5-ALA group. The relationships between different treatment regimens are described and summarized in Table 2.

As demonstrated in Figs. 4 and 5, the dose response curves were also collected using two-photon irradiation. The relationships between different treatment regimens are described and summarized in Table 3. It was noted that the dose response curves were consistent with the results obtained from the one-photon treatment, where CP-B cells were more susceptible to PpIX phototoxicity. In addition, because the focal volume of two-photon irradiation is much smaller than one-photon irradiation, the difference in viability of CP-B caused by PpIX was observed to be smaller than it was with one-photon treatment, as summarized in items c and d of Table 2. This was consistent with one-photon treatments for 5-ALA-stained HGD showing better efficacy than two-photon treatment when mitochondria were irradiated, as observed in Figs. 2 and 4 ($p < 0.05$). CP-A cells showed a similar viability between one- and two-photon regimes, which could be attributable to less intracellular PpIX concentration at 3 h of incubation (as mentioned in Fig. 1) or more resistance to the photosensitizing toxicity.

4 Discussion

In this study, subcellular irradiation of two BE cell lines was investigated as a potential *in vitro* model for "seek-and-treat" for esophageal dysplasia. It has also been demonstrated that the intracellular PpIX could serve as a contrast agent to highlight both types of esophageal cells (Fig. 1), while acting as a photosensitizer for selective treatment (Figs. 2 and 4). Image processing and classification have been performed in the coculture model that showed 95% sensitivity and 87% specificity for differentiating HGD based on these images.[31] The specific PDT efficacy achieved by subcellular irradiation was also characterized and correlated with the relative amount of intracellular PpIX activation and the light fluence applied to the cells. Using confocal fluorescence images of these cells, we found that both CP-B and CP-A cells achieved their maximum PpIX formation at mitochondria within 5 to 6 h, while the dysplastic cells (CP-B) demonstrated faster PpIX production than the metaplastic cells (CP-A), especially at 3 h of incubation (photon counts of 32 ± 3 in CP-B and 23 ± 3 in CP-A, $p < 0.01$).[31] Treatment was given and characterized at an earlier time frame (3 h); therefore, even if a false positive of detection occurs, it may not be harmful for the falsely treated metaplastic cells.

Correlating the discrepancy of intracellular PpIX to treatment efficacy, CP-B cells were found to be more susceptible to PpIX activation when different light fluence and subcellular treatment regimens were given. In contrast, both nonstained cell lines were observed to demonstrate similar viability when the same fluence was applied. According to the results from Figs. 2–5, comparison between groups and the corresponding explanations were summarized in Table 2. It is clear that the viability reduction between the 5-ALA groups and control (nonstained) groups was solely due to the photosensitizing effects from PpIX. This conclusion is further supported when comparing the

Table 2 The difference in cell viability between treatment regimes using one-photon PDT (5.92 J/cm^2).

Comparison	Viability		Notes
CP-A to PpIX	CP-$A_{PpIX\text{-}whole}$ 59%	CP-$A_{control\text{-}whole}$ 79%	−20% due to CP-A responses to PpIX[a]
	CP-$A_{PpIX\text{-}mito}$ 74%	CP-$A_{PpIX\text{-}nucleus}$ 77%	−3% (PpIX was partially activated)[b]
CP-B to PpIX	CP-$B_{PpIX\text{-}whole}$ 8%	CP-$B_{control\text{-}whole}$ 82%	−74% due to CP-B responses to PpIX[c]
	CP-$B_{PpIX\text{-}mito}$ 37%	CP-$B_{PpIX\text{-}nucleus}$ 72%	−35% (PpIX was partially activated)[d]
Cell sensitivity	CP-$B_{PpIX\text{-}whole}$ 8%	CP-$A_{PpIX\text{-}whole}$ 59%	CP-B is more sensitive to treatment[e]
	CP-$B_{PpIX\text{-}mito}$ 37%	CP-$A_{PpIX\text{-}mito}$ 74%	CP-B is more sensitive to treatment[f]
Cell to light fluence	CP-$A_{control\text{-}nucleus}$ 75%	CP-$A_{PpIX\text{-}nucleus}$ 77%	Laser effect dominates[g]
	CP-$B_{control\text{-}whole}$ 82%	CP-$A_{control\text{-}whole}$ 79%	Equivalent response to laser fluence[h]

Note: Superscripts a–h correspond to the items discussed in the main text.

Table 3 The difference in cell viability between treatment regimes using two-photon PDT (9911 J/cm^2).

Comparison	Viability		Notes
CP-A to PpIX	CP-$A_{PpIX\text{-}whole}$ 54%	CP-$A_{control\text{-}whole}$ 70%	−16% due to CP-A responses to PpIX[a]
	CP-$A_{PpIX\text{-}mito}$ 71%	CP-$A_{PpIX\text{-}nucleus}$ 81%	−10% (PpIX was partially activated)[b]
CP-B to PpIX	CP-$B_{PpIX\text{-}whole}$ 9%	CP-$B_{control\text{-}whole}$ 65%	−56% due to CP-B responses to PpIX[c]
	CP-$B_{PpIX\text{-}mito}$ 58%	CP-$B_{PpIX\text{-}nucleus}$ 87%	−29% (PpIX was partially activated)[d]
Cell sensitivity	CP-$B_{PpIX\text{-}whole}$ 9%	CP-$A_{PpIX\text{-}whole}$ 54%	CP-B is more sensitive to treatment[e]
	CP-$B_{PpIX\text{-}mito}$ 58%	CP-$A_{PpIX\text{-}mito}$ 71%	CP-B is more sensitive to treatment[f]
Cell to light fluence	CP-$A_{control\text{-}nucleus}$ 81%	CP-$A_{PpIX\text{-}nucleus}$ 84%	Laser effect dominates[g]
	CP-$B_{control\text{-}whole}$ 70%	CP-$A_{control\text{-}whole}$ 66%	Equivalent response to laser fluence[h]

Note: Superscripts a–h correspond to the items discussed in the main text.

viability between the nucleus treatment and mitochondrial treatment because the nucleus treatment irradiated the part "without PpIX." As shown in Table 2 from items a to d of one-photon irradiation, it was observed that the CP-B cells demonstrated 51% lower viability than CP-A cells after PpIX activation using whole cell irradiation. This was consistent with the comparison between 5-ALA incubated CP-A and CP-B cells with whole cell and mitochondrial irradiations (items e and f in Table 2). Although cell death was attributed to both photothermal and photochemical interactions, an additional 50% decrease in CP-B viability compared with CP-A cells may have been related to the discrepancy in intracellular PpIX intensity, where approximately 50% more PpIX intensity was observed in CP-B cells at 3 h of incubation, as mentioned in the previous paragraph. It should be noted that the difference in survival rate can also be affected by the intrinsic PDT resistance and sensitivity of CP-A and CP-B, respectively. However, CP-B viability is comparable with the previous 5-ALA-based cell study in a well-oxygenated environment.[33] Furthermore, equivalent cell responses to laser irradiation were found to be consistent between group comparisons as shown in items g and h of Table 2. The nucleus treatment on 5-ALA and nonstained groups caused no difference in viability, and the whole cell treatment between both no-drug controls also led to less than 5% difference in viability. Table 3 summarizes the results from two-photon PDT, which are similar to the one-photon irradiations except that the CP-B was less susceptible to the treatment, as PpIX was activated less efficiently. For instance, in items a and c of Table 3, CP-B only yielded an approximately 40% decrease in viability when compared with CP-A (16% versus 54%), which could also be partly attributed to the discrepancy of intracellular PpIX (23%)[31] and the intrinsic cell responses. The biological (cytotoxic) effect that is linearly proportional to the photosensitizer concentration was also in agreement with previous fluorescence-based studies on pharmacokinetics and localization of PpIX accumulation *in vivo*. In those studies, the PDT-induced necrosis was significantly greater in the control group and the intratissue PpIX fluorescence was correlated with the tissue damage after treatment.[34,35]

When comparing whole cell treatment with mitochondrial treatment on 5-ALA stained cells, it is necessary to account for the ratio of the photosensitized areas because only a partial activation was used in the mitochondrial treatment. We compared the ratio of the activated area and the corresponding changes in cell survival rate to obtain a more valid comparison of the two subcellular regimes. Table 4 showed the calculated values and standard deviation measured from multiple regions of interest, suggesting that both whole cell and partial mitochondrial treatments achieved comparable PDT efficacy although the whole cell treatment resulted in a lower survival rate due to additional energy deposition. Moreover, according to the treatment efficacy measured from the single-plane (thickness: one-photon ~0.8 μm; two-photon ~0.5 μm[36]) subcellular treatment at the fluence range, it is straightforward to come up with an assumption that one-photon excitation demonstrated a better killing efficacy as more PpIX along the light path was excited to induce the phototoxic effect. However, it should be noted that the photosensitizing effect would not be proportional to the fluence if the fluence rate applied to the sample depleted the ground state photosensitizers. The fluence rates used in this study were up to 0.12 W/cm^2 in one-photon treatment, which have negligible depletion effects on ground state photosensitizers in either high or low oxygen conditions.[37] On the other hand, two-photon excitation with the fluence rate of 96.8 W/cm^2 exceeded the reported limit, thus it was possible that the ground state photosensitizer was depleted during the treatment.[37]

PI was used as a necrotic stain to quantify cell death a short period of time after irradiation (2 h). It has been reported that apoptosis could be the main biological effect induced by PDT, although this depends on the cell type, overall dose, etc.[38,39] As

Table 4 Scaling factors for whole cell and mitochondrial treatments.

Groups	Fractional area (partial/total activation of PpIX)	Fractional changes in survival rate[a]
One-photon excitation	45% ± 11%[b]	47% ± 4%
Two-photon excitation		54% ± 11%

[a]Calculated using the ratios of item d to item c (Tables 2 and 3, values in "notes").
[b]Calculation from a single plane. The one-photon excitation volume will be further affected by the sample thickness.

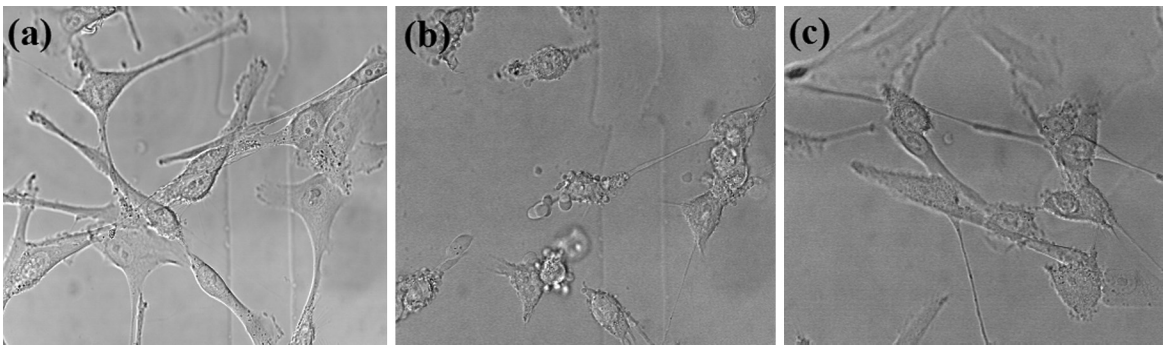

Fig. 6 Sample bright field images of 5-ALA loaded CP-B cells seeded on the glass-bottom dishes after exposure to various treatment regimes. (a) Cells remained the same morphology after exposed to the fluence level of imaging acquisition, suggesting a negligible adverse effect at this light dose; (b) CP-B cells were observed to exhibit necrotic cell death at 2 h after whole cell irradiation with the fluence of 5.92 J/cm^2; and (c) nucleus treatment on the 5-ALA loaded cells did not induce significant cell death when the mitochondria-localized PpIX was not activated.

the cell morphological features shown in Fig. 6, cells tended to demonstrate a necrotic cell death within 2 h after exposure to a high fluence. This phenomenon could be the consequence of PpIX-induced oxidative stress.[40] This agreed with a previous report that the oxidative stress-induced necrosis happens shortly after irradiation; the affected cells change the morphology in less than 1 h and go through necrosis within 2 h.[41]

5 Conclusion

In conclusion, the premalignant BE cell lines provide a platform to investigate detection and treatment strategies using a PDT photosensitizer. In addition to the distinct morphological patterns revealed by PpIX fluorescence imaging, this study demonstrated potential subcellular treatment strategies and their corresponding efficacies for cellular-based PDT, which will be an important component in real-time integrated detection and treatment of BE using endomicroscopic technology. Our results demonstrated that the HGD cells were less viable than metaplastic cells after PDT due to increased accumulation of PpIX at earlier times. More importantly, whole cell and mitochondrial treatments induced a comparable PDT effect, although the cell viability is different due to the fractional changes of the irradiated PpIX area. In contrast, nucleus irradiation only exhibited little phototoxicity. With the aid of automatic detection, this indicates that the appropriately targeted irradiation schemes directed at mitochondria may further enhance treatment selectivity without introducing excessive phototoxicity for non-HGD cells. Verifying these strategies in a coculture platform and three-dimensional cell cultures will be the logical next step complementary to quantitative imaging processing and classification.

Acknowledgments

This project is supported by funding from the Natural Sciences & Engineering Research Council (NSERC), Ontario Centres of Excellence (OCE), and Canadian Cancer Society (701734). The authors would like to thank Jennifer Bisson, Tahrin Mahmood, and Sharon Goh for their assistance in cell culture and sample preparation. SCY is supported in part by the NSERC Alexander Graham Bell Canada Graduate Scholarship and Ontario Graduate Scholarship (OGS). QF holds the Canada Research Chair in Biophotonics.

The authors have declared that no competing financial interest exists.

References

1. S. J. Spechler, "The natural history of dysplasia and cancer in Barrett's esophagus," *J. Clin. Gastroenterol.* **36**, 2–5 (2003).
2. C. J. Kelty, S. L. Marcus, and R. Ackroyd, "Photodynamic therapy for Barrett's esophagus: a review," *Dis. Esophagus* **15**, 137–144 (2002).
3. J. Rees et al., "Treatment for Barrett's oesophagus (Review)," in *Cochrane Collaboration*, John Wiley & Sons, Ltd., Etobicoke, Ontario, Canada (2011).
4. B. C. Wilson, "Detection and treatment of dysplasia in Barrett's esophagus: a pivotal challenge in translating biophotonics from bench to bedside," *J. Biomed. Opt.* **12**, 051401 (2007).
5. R. E. Sampliner, B. Fennerty, and H. S. Garewal, "Reversal of Barrett's esophagus with acid suppression and multipolar electrocoagulation: preliminary results," *Gastrointest. Endosc.* **44**, 532–535 (1996).
6. G. S. Dulai et al., "Randomized trial of argon plasma coagulation vs. multipolar electrocoagulation for ablation of Barrett's esophagus," *Gastrointest. Endosc.* **61**, 232–240 (2005).
7. A. Larghi et al., "EUS followed by EMR for staging of high-grade dysplasia and early cancer in Barrett's esophagus," *Gastrointest. Endosc.* **62**(1), 16–23 (2005).
8. P. K. Nijhawan and K. K. Wang, "Endoscopic mucosal resection for lesions with endoscopic features suggestive of malignancy and high-grade dysplasia within Barrett's esophagus," *Gastrointest. Endosc.* **52**, 328–332 (2000).
9. D. Mitton and R. Ackroyd, "Photodynamic therapy in oesophageal carcinoma: an overview. A brief history of photodynamic therapy," *Photochem. Photobiol. Sci.* **3**, 839–850 (2004).
10. C. J. Kelty et al., "The use of 5-aminolaevulinic acid as a photosensitiser in photodynamic therapy and photodiagnosis," *Photochem. Photobiol. Sci.* **1**, 158–168 (2002).
11. P. Hinnen et al., "Timing of 5-aminolaevulinic acid-induced photodynamic therapy for the treatment of patients with Barrett's oesophagus," *J. Photochem. Photobiol. B Biol.* **68**, 8–14 (2002).
12. T. D. Wang and J. Van Dam, "Optical biopsy: a new frontier in endoscopic detection and diagnosis," *Clin. Gastroenterol. Hepatol.* **2**, 744–753 (2004).
13. R. Kiesslich et al., "*In vivo* histology of Barrett's esophagus and associated neoplasia by confocal laser endomicroscopy," *Clin. Gastroenterol. Hepatol.* **4**, 979–987 (2006).
14. M. A. Kara et al., "Characterization of tissue autofluorescence in Barrett's esophagus by confocal fluorescence microscopy," *Dis. Esophagus* **20**, 141–150 (2007).
15. S.-C. A. Yeh et al., "Time-resolved fluorescence in photodynamic therapy," *Photonics* **1**, 530–564 (2014).

16. J. A. Russell et al., "Characterization of fluorescence lifetime of photofrin and delta-aminolevulinic acid induced protoporphyrin IX in living cells using single and two-photon excitation," *IEEE J. Quantum Electron.* **14**, 158–166 (2008).
17. A. Ruck et al., "SLIM: a new method for molecular imaging," *Microsc. Res. Tech.* **70**, 485–492 (2007).
18. M. C. A. Palanca-Wessels et al., "Extended lifespan of Barrett's esophagus epithelium transduced with the human telomerase catalytic subunit: a useful *in vitro* model," *Carcinogenesis* **24**, 1183–1190 (2003).
19. R. E. Kosoff et al., "Development and characterization of an organotypic model of Barrett's esophagus," *J. Cell. Physiol.* **227**, 2654–2659 (2012).
20. L. M. F. Merlo et al., "An in vitro co-culture model of esophageal cells identifies ascorbic acid as a modulator of cell competition," *BMC Cancer* **11**, 461–471 (2011).
21. K. B. Dunbar et al., "Confocal laser endomicroscopy in Barrett's esophagus and endoscopically inapparent Barrett's neoplasia: a prospective, randomized, double-blind, controlled, crossover trial," *Gastrointest. Endosc.* **70**, 645–654 (2009).
22. M. I. Canto, "Endomicroscopy of Barrett's esophagus," *Gastroenterol. Clin. North Am.* **39**, 759–769 (2010).
23. P. Hinnen, *Biochemical aspects of ALA-PDT basic mechanisms and optimization for the treatment of Barrett's oesophagus*, Erasmus University Rotterdam, Rotterdam (2001).
24. J. C. Kennedy, R. H. Pottier, and D. C. Pross, "Photodynamic therapy with endogenous protoporphyrin IX: basic principles and present clinical experience," *J. Photochem. Photobiol. B* **6**, 143–148 (1990).
25. P. E. Claydon and R. Ackroyd, "5-Aminolaevulinic acid-induced photodynamic therapy and photodetection in Barrett's esophagus," *Dis. Esophagus* **17**, 205–212 (2004).
26. C. J. Kelty et al., "Comparison of high- vs low-dose 5-aminolevulinic acid for photodynamic therapy of Barrett's esophagus," *Surg. Endosc.* **18**, 452–458 (2004).
27. R. Ackroyd et al., "5-aminolevulinic acid photosensitization of dysplastic Barrett's esophagus: a pharmacokinetic study," *Photochem. Photobiol.* **70**, 656–662 (1999).
28. C. J. Kelty et al., "Endoscopic ablation of Barrett's oesophagus: a randomized-controlled trial of photodynamic therapy vs. argon plasma coagulation," *Aliment. Pharmacol. Ther.* **20**, 1289–1296 (2004).
29. R. L. P. van Veen et al., "*In situ* light dosimetry during photodynamic therapy of Barrett's esophagus with 5-aminolevulinic acid," *Lasers Surg. Med.* **31**, 299–304 (2002).
30. H. C. Wolfsen, "Present status of photodynamic therapy for high-grade dysplasia in Barrett's esophagus," *J. Clin. Gastroenterol.* **39**, 189–202 (2005).
31. S.-C. A. Yeh et al., "5-ALA induced PpIX as a fluorescence marker for quantitative image analysis of high-grade dysplasia in Barrett's esophagus cellular models," *J. Biomed. Opt.* (submitted) (2014).
32. M. C. A. Palanca-Wessels et al., "Genetic analysis of long-term Barrett's esophagus epithelial cultures exhibiting cytogenetic and ploidy abnormalities," *Gastroenterology* **114**, 295–304 (1998).
33. J. S. Dysart and M. S. Patterson, "Photobleaching kinetics, photoproduct formation, and dose estimation during ALA induced PpIX PDT of MLL cells under well oxygenated and hypoxic conditions," *Photochem. Photobiol. Sci.* **5**, 73–81 (2006).
34. A. Johansson et al., "5-Aminolevulinic acid-induced protoporphyrin IX levels in tissue of human malignant brain tumors," *Photochem. Photobiol.* **86**, 1373–1378 (2010).
35. P. A. Valdes et al., "5-aminolevulinic acid-induced protoporphyrin IX concentration correlates with histopathologic markers of malignancy in human gliomas: the need for quantitative fluorescence-guided resection to identify regions of increasing malignancy," *Neuro-oncology* **13**(8), 846–856 (2011).
36. W. R. Zipfel, R. M. Williams, and W. W. Webb, "Nonlinear magic: multiphoton microscopy in the biosciences," *Nat. Biotechnol.* **21**, 1369–1377 (2003).
37. M. A. Weston and M. S. Patterson, "Monitoring oxygen concentration during photodynamic therapy using prompt photosensitizer fluorescence," *Phys. Med. Biol.* **58**, 7039–7059 (2013).
38. D. Kessel et al., "The role of subcellular localization in initiation of apoptosis by photodynamic therapy," *Photochem. Photobiol.* **65**, 422–426 (1997).
39. N. L. Oleinick, R. L. Morris, and I. Belichenko, "The role of apoptosis in response to photodynamic therapy: what, where, why, and how," *Photochem. Photobiol. Sci.* **1**, 1–21 (2002).
40. C. H. Kim et al., "Effect of 5-aminolevulinic acid-based photodynamic therapy via reactive oxygen species in human cholangiocarcinoma cells," *Int. J. Nanomed.* **6**, 1357–1363 (2011).
41. T. Vanden Berghe et al., "Necroptosis, necrosis and secondary necrosis converge on similar cellular disintegration features," *Cell Death Differ.* **17**, 922–930 (2009).

Shu-Chi Allison Yeh received a BSc degree in physiotherapy from Chung Shan Medical University in Taiwan in 2007 and completed a PhD in biomedical engineering from McMaster University, Hamilton, ON, Canada, in 2015. Her research interests include applications of steady-state and time-resolved fluorescence microscopy, and intravital imaging for diagnosis and treatment of cancer.

David W. Andrews is director and senior scientist, Biological Sciences, Sunnybrook Research Institute. His research interests include cancer research, regulation of apoptosis by Bcl-2 family proteins, high content screening and the development of new fluorescence microscopes to measure protein:protein interactions in live cells. He is an active member of journal editorial boards, consults in the private sector, is on several scientific advisory boards, holds licensed patents, and has participated in several start-up companies.

Michael Patterson received a BSc in physics from Queen's University in 1973 and an MSc in applied nuclear physics from McMaster University in 1976. After working for four years as a medical physicist, he returned to graduate school and earned his PhD in medical biophysics from the University of Toronto for his research in ultrasonic imaging. Since joining the Juravinski Cancer Centre and McMaster in 1984, his research has focused on optical methods for diagnosis and treatment of cancer.

Joseph E. Hayward obtained his PhD from the Department of Engineering Physics at McMaster University. He is a medical physicist at the Juravinski Cancer Centre in Hamilton, Ontario. His current research interests include optical methods of monitoring radiation induced toxicities and non-invasive strategies to identify the margins of malignant skin lesions. He is an associate professor in the Departments of Radiology and Medical Physics and Applied Radiation Sciences at McMaster University.

Qiyin Fang is an associate professor of engineering physics at McMaster University and holds the Canada Research Chair in Biophotonics. He is a member of the McMaster School of Biomedical Engineering. His current research interests include steady-state and time-resolved fluorescence spectroscopy/imaging for biomedical applications, e.g., optical biopsy, wide-field imaging, endoscopy and microscopy. He obtained his master's and doctoral degrees from East Carolina University and his undergraduate degree from Nankai University.

Biographies of the other authors are not available.